



Cite this: *Dalton Trans.*, 2019, **48**, 2896

Received 16th January 2019,

Accepted 6th February 2019

DOI: 10.1039/c9dt00228f

rsc.li/dalton

Reversible O–H bond activation by an intramolecular frustrated Lewis pair†

Petra Vasko, ^{a,b} M. Ángeles Fuentes, ^a Jamie Hicks^a and Simon Aldridge ^{a*}

The interactions of the O–H bonds in alcohols, water and phenol with dimethylxanthene-derived frustrated Lewis pairs (FLPs) have been probed. Within the constraints of this backbone framework, the preference for adduct formation or O–H bond cleavage to give the corresponding zwitterion is largely determined by pK_a considerations. In the case of the $PPh_2/B(C_6F_5)_2$ system and p - t -BuC₆H₄OH, an equilibrium is established between the two isomeric forms which allows the thermodynamic parameters associated with zwitterion formation *via* O–H bond cleavage to be probed.

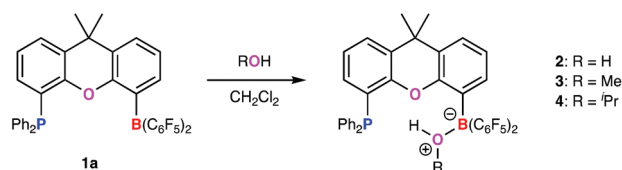
In recent years, frustrated Lewis pairs (FLPs) have emerged as an attractive new approach in the fields of small molecule activation and catalysis;¹ reports of the use of FLPs in the heterolytic cleavage of dihydrogen and other E–H bonds (E = C, N, O, Si, B) continue to rise year-on-year. By extension ‘metal-free’ approaches for carrying out bond modification reactions using FLPs have evolved from proof-of-concept to an active research field in main group catalysis. Most notably, FLP-catalysed hydrogenation reactions have been successfully deployed for a wide range of functional groups, including imines, aldehydes, ketones, alkenes and alkynes.²

We have previously shown that the dimethylxanthene backbone provides a versatile scaffold for intramolecular FLPs (*e.g.* **1a**; Scheme 1); the separation between the Lewis acid and base components typically lies between 4.0 and 4.5 Å and is therefore pre-organised for the activation of small molecules such as H₂.⁴ Recently we also showed that FLP **1a** reacts readily with the C–H bonds in terminal alkynes and with the B–H bonds in

selected boranes, and can act as a pre-catalyst for the hydroboration of alkynes.⁵

In terms of other E–H bonds, the interactions of FLPs with water and O–H containing systems are important,^{6–13} not least because they influence strongly their sensitivity to trace impurities present in commercial substrates and solvents; as a consequence, it is often necessary to carry out catalytic processes under the exclusion of moisture. Similar chemistry potentially arises when using alcohol solutions in combination with FLPs as alcohols can have comparable nucleophilicity/basicity to H₂O.³ With these issues in mind, we set out to investigate the reactivity of FLP **1a** (and related systems) towards common O–H bond containing substrates, namely water, alcohols and phenols.

The reactions of FLP **1a** with excess water or methanol/2-propanol in dichloromethane result in a gradual colour change from a bright yellow to colourless (Scheme 1 and ESI†). The products of these reactions (**2–4**) can be crystallized from dichloromethane/hexane and their solid-state structures determined crystallographically. These confirm that **1a** assimilates one equivalent of ROH (R = H (**2**), Me (**3**) or ^{*i*}Pr (**4**)) to form the respective O-bound adduct (Fig. 1). In each case, the ROH fragment is bonded to B(1), rendering the boron centre tetrahedral and O(2) trigonal pyramidal. The O–H proton(s) in each case could be located in the difference Fourier map and refined without restraints. The B(1)–O(2) distances fall in the range 1.595(3)–1.611(2) Å, which are comparable to previously reported borane adducts of water/alcohols.^{6–11}



Scheme 1 Reactions of FLP **1a** with water, methanol and 2-propanol.

^aDepartment of Chemistry, University of Oxford, Inorganic Chemistry Laboratory, South Parks Road, Oxford, OX1 3QR, UK. E-mail: petra.vasko@chem.ox.ac.uk, simon.aldrige@chem.ox.ac.uk

^bDepartment of Chemistry, Nanoscience Center, University of Jyväskylä, P. O. Box 35, Jyväskylä, FI-40014, Finland

† Electronic supplementary information (ESI) available: Experimental and computational details, X-ray crystallographic and characterisation data. CCDC 1872780–1872784. For ESI and crystallographic data in CIF or other electronic format see DOI: 10.1039/c9dt00228f

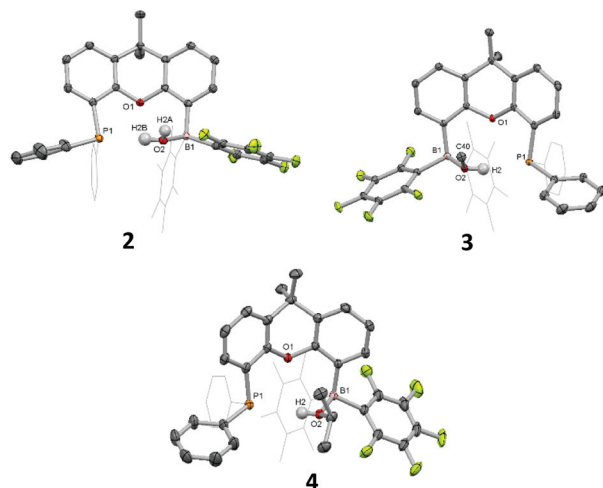
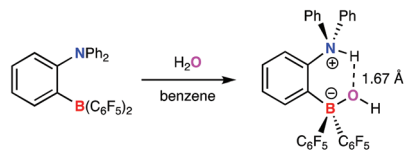


Fig. 1 Molecular structures of **2**, **3** and **4**. Parts of the FLPs are shown in a wireframe format, and solvent molecules and most hydrogen atoms are omitted for clarity. Thermal ellipsoids are drawn at 40% probability. Selected bond lengths (Å) and angles (°): **2**: B1–O2 1.611(2), O2–H2A 0.76(3), O2–H2B 0.92(3), P1–H2B 2.32(3), B1–O2–P1 115.7(1); **3**: B1–O2 1.596(2), O2–H2 0.91(2), P1–H2 2.25(2), B1–O2–P1 115.3(1); **4**: B1–O2 1.595(4), O2–H2 0.82(3), P1–H2 2.49(3), B1–O2–P1 112.4(1).

Further support for the assignment of **2–4** as simple Lewis adducts can be obtained from solution state NMR studies. The ^1H NMR spectra of **2** and **4** show broad singlets for the O-bound proton(s) at 8.10 and 9.17 ppm, respectively. In the case of **3**, the corresponding ^1H NMR signal (at 10.80 ppm) is actually a doublet, although the coupling constant ($J_{\text{PH}} = 16.8$ Hz) is significantly smaller than that expected for a direct P–H bond in systems of this type (>500 Hz; *vide infra*). In similar fashion, the respective proton-coupled ^{31}P NMR spectra feature singlet resonances in each case (at *ca.* -20 ppm) rather than the wide doublet expected for a *bona fide* P–H single bond. The boron centre in each adduct gives rise to a broad signal in the $^{11}\text{B}\{^1\text{H}\}$ spectrum in the range characteristic of four-coordinate boron species ($\delta_{\text{B}} = 4.5$ (**2**), 5.4 (**3**), and 3.7 ppm (**4**)), consistent with the solid state structures.⁵

Earlier literature reports detailing the reactivity of FLPs towards water favour heterolytic O–H bond cleavage;^{6–11} for example the $^t\text{Bu}_3\text{P/B}(\text{C}_6\text{F}_5)_3$ system is reported to activate one molecule of H_2O to give the phosphonium borate $[\text{Bu}_3\text{PH}][(\text{HO})\text{B}(\text{C}_6\text{F}_5)_3]$.⁷ The difference in this system compared to **1a** can be understood (primarily) in terms of the relative basicities of the two phosphine components. More difficult to rationalize based on simple pK_{a} values is the contrasting behaviour of **1a** and $1,2\text{-C}_6\text{H}_4(\text{NPh}_2)\{\text{B}(\text{C}_6\text{F}_5)_2\}$;⁶ the latter has been shown to deprotonate the bound H_2O molecule (to give a zwitterionic anilinium borate) despite the fact that systems of the type ArNPh_2 are typically very weak Brønsted bases (Scheme 2).¹⁴

Presumably, the difference relates to the presence of a strong intramolecular N–H \cdots O hydrogen bond (which is



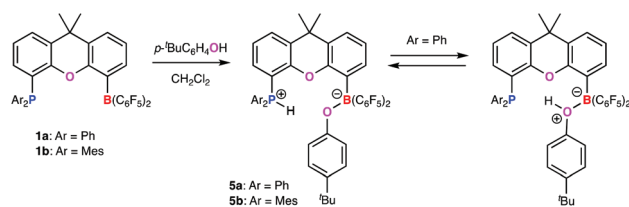
Scheme 2 O–H bond cleavage in water by Roesler and Piers' aniline/borane FLP.⁶

reported to feature an O \cdots H contact shorter than those in water) of a type which is precluded in the putative analogue derived from **1a**, on the basis of the greater separation of the Lewis acid and base components. The P \cdots O separation associated with the bound water molecule in **2** is $3.237(2)$ Å.

Reasoning that the use of a more acidic O–H bond might bring about O–H bond cleavage, we investigated the reactions of **1a** (and the related $-\text{PMes}_2$ derivative **1b**) with phenols; $p\text{-}^t\text{BuC}_6\text{H}_4\text{OH}$ was chosen given the presence of the ^tBu group as a convenient ^1H NMR handle. Accordingly, the reaction between **1a** and excess $p\text{-}^t\text{BuC}_6\text{H}_4\text{OH}$ in dichloromethane leads to immediate discharge of the yellow colour of the FLP; filtration, concentration and layering with *n*-hexane yielded colourless single crystals suitable for X-ray diffraction studies.

The molecular structure shows that **1a** reacts with one equivalent of the phenol to give the (O–H activated) phosphonium borate zwitterion **5a** (Scheme 3 and Fig. 2). The P-bound proton H(1) could be located in the difference Fourier map and refined without restraints. With the usual caveats concerning the location of hydrogen atoms by X-ray methods, there appears to be little residual interaction between H(1) and O(2) ($d(\text{H}(1)\text{--O}(2)) = 2.19(1)$ Å *cf.* $d(\text{P}(1)\text{--H}(1)) = 1.28(2)$ Å). The location of the hydrogen atom at P(1) is also consistent with the observed widening of the C–P–C angles in **5a** compared to **1a** itself ($108.5(1)\text{--}112.6(1)^\circ$ *cf.* $101.4(1)\text{--}102.7(1)^\circ$).

Intriguingly, however, a solution made by re-dissolving crystals of **5a** in benzene- d_6 features a *singlet* resonance in the ^1H spectrum at $\delta_{\text{H}} = 9.69$ ppm, and in the proton-coupled ^{31}P NMR spectrum (at $\delta_{\text{P}} = -13.0$ ppm). These signals contrast markedly with the wide doublet resonances typically associated with P–H groups in systems of this sort (*vide infra*). In addition, the ^{19}F NMR signals associated with the boron-bound C_6F_5 groups in **5a** are more consistent with a neutral borane adduct $\text{RO}(\text{H})\text{--BAr}(\text{C}_6\text{F}_5)_2$ than an anionic system of the type $[\text{RO--BAr}(\text{C}_6\text{F}_5)_2]^-$. In particular, the separation between the resonances associated with the *meta* and *para* CF groups ($\Delta\delta_{m,p} = 6.5$ ppm) is similar to those measured for water/



Scheme 3 Reactions of FLPs **1a** and **1b** with $p\text{-}^t\text{BuC}_6\text{H}_4\text{OH}$.



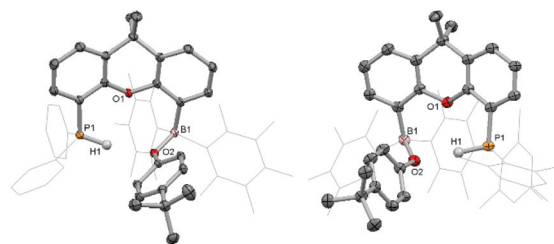


Fig. 2 Molecular structures of **5a** (left) and **5b** (right). Parts of the FLPs are shown in a wireframe format, solvent molecules and most hydrogen atoms are omitted for clarity. Thermal ellipsoids are drawn at 40% probability. Selected bond lengths (Å) and angles (°): **5a**: B1–O2 1.495(1), P1–H1 1.28(2), O2–H1 2.19(1), P1–O2 3.458(1), C2–P1–C16 108.1(1), C2–P1–C22 112.6(1), C16–P1–C22 109.3(1); **5b**: B1–O2 1.498(3), P1–H1 1.39(3), O2–H1 2.31(3), P1–O2 3.615(2), C2–P1–C16 106.0(1), C2–P1–C25 116.8(1), C16–P1–C25 112.4(1).

alcohol adducts **2–4** (7.5–8.0 ppm). These observations suggest that **5a** adopts a different structure in solution to the zwitterionic form seen in the solid state – namely a simple donor/acceptor adduct akin to **2–4**.

With this apparent inconsistency in mind, we carried out variable temperature NMR measurements on **5a** in dichloromethane- d_2 . Cooling the sample to 257 K results in the appearance of a well-resolved doublet in the ^{31}P NMR spectrum at $\delta_{\text{P}} = -11.9$ ppm ($^1J_{\text{PH}} = 554$ Hz) and a change in the low-field part of the ^1H NMR spectrum, with a complementary doublet appearing at $\delta_{\text{H}} = 10.48$ ppm. The ^{19}F NMR spectrum in the low temperature limit is characterized by a reduced value of $\Delta\delta_{\text{m,p}}$ (4.9 ppm), similar to that measured for the related PMes_2 system (4.2 ppm) which adopts the zwitterionic O–H activated structure under all conditions examined (*vide infra*). These changes are reversible, and are consistent with an equilibrium involving isomeric species related through O–H bond cleavage; the solution-phase structure of **5a** at low temperatures resembles the zwitterion found in the solid state, while at higher temperatures a structure similar to those determined for adducts **2–4** predominates. A van't Hoff analysis carried out in CD_2Cl_2 at temperatures in the range 259–281 K allows for the determination of the enthalpic ($\Delta H^\circ = -69$ kJ mol $^{-1}$) and entropic terms ($\Delta S^\circ = -201$ J mol $^{-1}$ K $^{-1}$) associated with O–H bond breakage in this equilibrium. The relatively large magnitude of ΔS° is consistent with the narrow temperature window over which the transformation occurs, and reflects the more ordered nature of the zwitterionic form and its influence on the solvent sphere (presumably driven by electrostatic considerations).

To complement these experimental studies, we also sought to probe the thermodynamics of the two structural isomers of **5a** computationally by DFT. Both the Lewis adduct and zwitterionic forms were optimized using the PBE1PBE hybrid exchange–correlation functional in combination with Def-TZVP basis set;¹⁵ we also included a polarizable continuum model¹⁶ (PCM, dichloromethane) to describe the difference in optimized energies of the two isomers more accurately. The

computed free energies show that the adduct represents the more stable structure at 298 K, but only by 8.3 kJ mol $^{-1}$. We were also able to locate a transition state for the migration of the proton at 9.2 kJ mol $^{-1}$ in dichloromethane. These calculated values are consistent with our experimental findings and confirm the lability of the O–H bond in **5a**; proton transfer occurs very readily and the solid-state structure is presumably stabilised by favourable packing forces relating to its greater degree of charge separation.

For comparison we also wanted to examine the reactivity of $p\text{-}^t\text{BuC}_6\text{H}_4\text{OH}$ towards the related FLP **1b**, which features PMes_2 ($\text{Mes} = \text{C}_6\text{H}_2\text{-2,4,6-Me}_3$), rather than PPh_2 as the Lewis basic component.⁴ We hypothesized that the enhanced basicity of the phosphine donor would bias the thermodynamics of O–H bond cleavage in favour of the zwitterionic form. The reaction between **1b** and excess $p\text{-}^t\text{BuC}_6\text{H}_4\text{OH}$ proceeds instantly and the molecular structure of the product, **5b**, can be shown by X-ray crystallography to be closely related to that of **5a** (Fig. 2). Electron density close to P(1) and the geometry of the C_3P heavy atom skeleton strongly suggest the presence of a P–H bond. Importantly – in this case – the solid state-structure appears to be retained in solution at all temperatures. Thus, both the proton coupled ^{31}P and ^1H spectra at room temperature feature a doublet with $^1J_{\text{PH}} = 542$ Hz ($\delta_{\text{P}} = -27.3$ ppm; $\delta_{\text{H}} = 9.74$ ppm). Consistently, DFT structural optimisations show that the zwitterionic form of **5b** is more stable than the corresponding adduct by 34.6 kJ mol $^{-1}$ in dichloromethane.

In conclusion, we have studied the interactions of the O–H bonds in alcohols, water and phenol with the dimethyl-xanthene based FLPs **1a** and **1b**. Within the constraints of this particular intramolecular framework, the preference for adduct formation or O–H cleavage to give the corresponding zwitterion is largely determined by pK_{a} considerations. In the case of the **1a**/ $p\text{-}^t\text{BuC}_6\text{H}_4\text{OH}$ system, an equilibrium is established between the two isomeric forms which allows the thermodynamic parameters associated with O–H activation to be probed.

Conflicts of interest

There are no conflicts to declare.

Acknowledgements

We would like to thank the Advanced Research Computing (ARC) facilities for providing computational resources and Dr Nick Rees for help with the NMR experiments. PV would like to thank the Magnus Ehrnrooth and Finnish Cultural Foundations for funding. MAF would like to thank the EPSRC for funding (EP/K014714/1)

Notes and references

- (a) G. C. Welch, R. R. San Juan, J. D. Masuda and D. W. Stephan, *Science*, 2006, **314**, 1124; (b) D. W. Stephan



- and G. Erker, *Angew. Chem., Int. Ed.*, 2015, **54**, 6400; (c) D. J. Scott, M. J. Fuchter and A. E. Ashley, *Chem. Soc. Rev.*, 2017, **46**, 5689.
- 2 (a) D. W. Stephan, *J. Am. Chem. Soc.*, 2015, **137**, 10018; (b) D. W. Stephan, *Science*, 2016, **354**, aaf7229; (c) S. Tussing, K. Kaupmees and J. Paradies, *Chem. – Eur. J.*, 2016, **22**, 7422; (d) K. Chernichenko, Á. Madarasz, I. Pápai, M. Nieger, M. Leskelä and T. Repo, *Nat. Chem.*, 2013, **5**, 718; (e) D. J. Scott, M. J. Fuchter and A. E. Ashley, *J. Am. Chem. Soc.*, 2014, **136**, 15813.
- 3 (a) V. Fasano and M. J. Ingleson, *Synthesis*, 2018, **50**, 1783; (b) D. J. Scott, T. R. Simmons, E. J. Lawrence, G. G. Wildgoose, M. J. Fuchter and A. E. Ashley, *ACS Catal.*, 2015, **5**, 5540; (c) J. W. Thomson, J. A. Hatnean, J. J. Hastie, A. Pasternak, D. W. Stephan and P. A. Chase, *Org. Process Res. Dev.*, 2013, **17**, 1287.
- 4 (a) Z. Mo, E. L. Kolychev, A. Rit, J. Campos, H. Niu and S. Aldridge, *J. Am. Chem. Soc.*, 2015, **137**, 12227; (b) Z. Mo, A. Rit, J. Campos, E. L. Kolychev and S. Aldridge, *J. Am. Chem. Soc.*, 2016, **138**, 3306.
- 5 P. Vasko, I. A. Zulkifly, M. Á. Fuentes, Z. Mo, J. Hicks, P. C. J. Kamer and S. Aldridge, *Chem. – Eur. J.*, 2018, **24**, 10531.
- 6 R. Roesler, W. E. Piers and M. Parvez, *J. Organomet. Chem.*, 2003, **680**, 218.
- 7 (a) M. Klahn, A. Spannenberg and U. Rosenthal, *Acta Crystallogr., Sect. E: Struct. Rep. Online*, 2012, **68**, o1549; (b) G. Ghattas, C. Bizzarri, M. Hölscher, J. Langanke, C. Gürtler, W. Leitner and M. A. Subhani, *Chem. Commun.*, 2017, **53**, 3205.
- 8 C. Bergquist, B. M. Bridgewater, C. J. Harlan, J. R. Norton, R. A. Friesner and G. Parkin, *J. Am. Chem. Soc.*, 2000, **122**, 10581.
- 9 A. Di Saverio, F. Focante, I. Camurati, L. Resconi, T. Beringhelli, G. D'Alfonso, D. Donghi, D. Maggioni, P. Mercandelli and A. Sironi, *Inorg. Chem.*, 2005, **44**, 5030.
- 10 T. Wang, G. Kehr, L. Liu, S. Grimme, C. G. Daniliuc and G. Erker, *J. Am. Chem. Soc.*, 2016, **138**, 4302.
- 11 D. J. Scott, N. A. Phillips, J. S. Sapsford, A. C. Deacy, M. J. Fuchter and A. E. Ashley, *Angew. Chem., Int. Ed.*, 2016, **55**, 14738.
- 12 T. Xu and E. Y.-X. Chen, *J. Am. Chem. Soc.*, 2014, **136**(5), 1774.
- 13 M. J. Drewitt, M. Niedermann and M. C. Baird, *Inorg. Chim. Acta*, 2002, **340**, 207.
- 14 See, for example, http://evans.rc.fas.harvard.edu/pdf/evans_pka_table.pdf; retrieved 15/01/19.
- 15 (a) J. P. Perdew, K. Burke and M. Ernzerhof, *Phys. Rev. Lett.*, 1996, **77**, 3865; (b) J. P. Perdew, M. Ernzerhof and K. Burke, *J. Chem. Phys.*, 1996, **105**, 9982; (c) C. Adamo and V. Barone, *J. Chem. Phys.*, 1999, **110**, 6158; (d) J. P. Perdew, K. Burke and M. Ernzerhof, *Phys. Rev. Lett.*, 1997, **78**, 1396; (e) A. Schaefer, C. Huber and R. Ahlrichs, *J. Chem. Phys.*, 1994, **100**, 5829.
- 16 J. Tomasi, B. Mennucci and R. Cammi, *Chem. Rev.*, 2005, **105**, 2999.

